

# Motion Avatar: Generate Human and Animal Avatars with Arbitrary Motion

Zeyu Zhang<sup>12\*†</sup>

<https://steve-zeyu-zhang.github.io>

Jiran Wang<sup>2\*</sup>

[w0709256@anu.edu.au](mailto:w0709256@anu.edu.au)

Biao Wu<sup>3\*</sup>

[biaowu165534@gmail.com](mailto:biaowu165534@gmail.com)

Shuo Chen<sup>4</sup>

[sche0236@student.monash.edu](mailto:sche0236@student.monash.edu)

Zhiyuan Zhang<sup>5</sup>

[sjnns5995@gmail.com](mailto:sjnns5995@gmail.com)

Shiya Huang<sup>5</sup>

[shiya.huang@student.adelaide.edu.au](mailto:shiya.huang@student.adelaide.edu.au)

Wenbo Zhang<sup>5</sup>

[wenbo.zhang01@adelaide.edu.au](mailto:wenbo.zhang01@adelaide.edu.au)

Meng Fang<sup>6</sup>

[meng.fang@liverpool.ac.uk](mailto:meng.fang@liverpool.ac.uk)

Ling Chen<sup>3</sup>

[ling.chen@uts.edu.au](mailto:ling.chen@uts.edu.au)

Yang Zhao<sup>1✉</sup>

<https://yangyangkiki.github.io>

<sup>1</sup> La Trobe University

Bundoora VIC, Australia

<sup>2</sup> The Australian National University

Canberra ACT, Australia

<sup>3</sup> University of Technology Sydney

Ultimo NSW, Australia

<sup>4</sup> Monash University

Clayton VIC, Australia

<sup>5</sup> The University of Adelaide

Adelaide SA, Australia

<sup>6</sup> The University of Liverpool

Liverpool, United Kingdom

\*Equal contribution.

✉Corresponding author.

†Work done while being a research assistant at La Trobe University.

Project Website: <https://steve-zeyu-zhang.github.io/MotionAvatar>

## Abstract

In recent years, there has been significant interest in creating 3D avatars and motions, driven by their diverse applications in areas like film-making, video games, AR/VR, and human-robot interaction. However, current efforts primarily concentrate on either generating the 3D avatar mesh alone or producing motion sequences, with integrating these two aspects proving to be a persistent challenge. Additionally, while avatar and motion generation predominantly target humans, extending these techniques to animals remains a significant challenge due to inadequate training data and methods. To bridge these gaps, our paper presents three key contributions. Firstly, we proposed a novel agent-based approach named **Motion Avatar**, which allows for the automatic generation of high-quality customizable human and animal avatars with motions through text queries. The method significantly advanced the progress in dynamic 3D character generation. Secondly, we introduced a **LLM planner** that coordinates both motion and avatar generation, which transforms a discriminative planning into a customizable Q&A fashion. Lastly, we presented an animal motion dataset named **Zoo-300K**, comprising approximately **300,000**

text-motion pairs across 65 animal categories and its building pipeline **ZooGen**, which serves as a valuable resource for the community.

## 1 Introduction

The field of computational modeling for dynamic 3D or 4D avatars holds significant importance across various domains such as robotics, virtual, and augmented reality, computer gaming, and multimedia. Creating high-quality and user-friendly animated avatars is a desired goal of the 3D computer vision community. This involves not only ensuring the visual appeal of the avatars but also prioritizing their functionality and ease of use. Traditional methods [14, 27, 62] involve extracting information directly from video recordings, then using the data to model and reconstruct dynamic avatars in both spatial and temporal dimensions. Other approaches [67] involve integrating 3D reconstruction with video diffusion to bring 3D meshes to life through animation. However, these methods often suffer from imprecise and limited motion control, or exhibit inconsistencies between multiple views of the 3D mesh. These limitations hinder the seamless manipulation and other real world applications of dynamic avatars in interactive settings.

Recent advancements in *text-to-motion* generation [10, 18, 20, 53, 66], employing both diffusion [12, 21, 54, 46, 50] and autoregressive [42, 56] models, have demonstrated significant promise. These advancements represent a notable step forward in generating motion sequences directly from textual descriptions, which brings a new approach to dynamic motion avatar generation. Meanwhile, significant advancements in 3D mesh reconstruction and generation [23, 29, 30, 40, 54], particularly through approach of *image-to-3D*, have demonstrated considerable promise and dominance in the field of 3D object reconstruction. These advancements hold great potential for real-world applications. However, existing efforts predominantly focus on either creating the 3D avatar mesh independently or generating motion sequences separately. Yet, effectively integrating these two components remains a persistent challenge.

Moreover, although avatar and motion generation techniques are primarily developed for human characters, their adaptation to animals presents a formidable obstacle. This challenge arises primarily from the scarcity of suitable training data and the limitations of existing methodologies. Expanding these technologies to encompass animal characters requires novel approaches and a deeper understanding of animal behavior and anatomy [51].

Therefore, in order to address these challenges, our study delineates three principal contributions as follows:

- Firstly, we introduced a groundbreaking method named **Motion Avatar**, which leverages LLM agent-based techniques to automatically create customizable human and animal avatars complete with dynamic motions based on text input. This innovation represents a significant leap forward in the field of dynamic 3D character generation, offering high-quality avatars tailored to specific needs and preferences. With Motion Avatar, users can effortlessly generate lifelike characters with realistic movements, pushing the boundaries of what’s achievable in avatar creation through textual condition.
- Secondly, we introduced a **LLM planner** that handles both motion and avatar generation. This planner takes a discriminative planning approach and refines it into a more flexible Q&A paradigm. The generalization ability of the LLM planner will help adapt to broader dynamic avatar generation tasks in the future.

- Lastly, we presented a comprehensive animal motion dataset called **Zoo-300K**, which contains around **300,000** pairs of text descriptions and corresponding motion data covering **65** different animal categories. Additionally, we developed **ZooGen**, a robust pipeline for constructing such datasets, which stands as a valuable asset for the wider research community.

## 2 Related Works

**Text-to-Motion Generation** Creating motion is a vital aspect of computer vision, playing a crucial role in diverse applications such as 3D video animation, computer games, and robot manipulation. A prevalent approach to generating motion, known as the *Text-to-Motion* task, revolves around establishing a shared latent space for both textual descriptions and motion data. Among these applications, human motion generation has garnered significant attention and exploration. MotionCLIP [62] leverages Transformer-based [56] Autoencoders to reconstruct motion sequences while ensuring alignment with corresponding textual labels within the CLIP [44] space. This alignment effectively integrates semantic knowledge from CLIP into the manifold of human motion. TEMOS [67] and T2M [18] merge a Transformer-based Variational Autoencoder (VAE) [25] with a text encoder to produce distribution parameters that operate within the latent space of the VAE. AttT2M [68] and TM2D [15] integrate a body-part spatio-temporal encoder into VQ-VAE to facilitate improved learning of a discrete latent space with heightened expressiveness. MotionDiffuse [64] presents a pioneering framework for generating motion guided by text, leveraging diffusion models [12, 21, 64, 46, 50]. It demonstrates various appealing traits such as probabilistic mapping, lifelike synthesis, and multi-tiered manipulation. Conversely, MDM [63] employs a Transformer-based diffusion model devoid of classifiers to forecast samples, rather than noise, at each step. In contrast, MLD [10] conducts diffusion within latent motion space, eschewing the utilization of a diffusion model to forge links between raw motion sequences and conditional inputs. Motion Mamba [66] and InfiniMotion [65] proposed approaches which leveraged state space models (SSMs) [16] and diffusion to design an efficient architecture for long-sequence human motion generation. MoMask [20] proposed a novel masked modeling framework, designed a hierarchical quantization scheme architecture, and achieved superior results on text-driven 3D human motion generation.

Currently, generating animal motion possesses greater challenges compared to human motion generation. These challenges primarily stem from inadequate data and inconsistent motion representation, such as variations in the number of joints and kinematics. Nevertheless, there are ongoing efforts aimed at addressing these hurdles. OmniMotionGPT [60] proposes a method for generating diverse and realistic animal motion sequences from textual descriptions, achieving superior results compared to traditional human motion synthesis approaches, by leveraging a model architecture inspired by GPT [3, 9, 42, 43] and joint training of motion autoencoders for both animal and human motions. SinMDM [40] introduced a method for synthesizing diverse motions of arbitrary length from a single input motion sequence, addressing the scarcity of data instances in animating animals and exotic creatures, and outperformed existing methods in quality and efficiency.

**Avatar Generation** Previously, research on 3D avatar and texture generation has drawn inspiration from text-guided 2D image generation techniques. Typically, these methods involve either training a normalizing flow model based on textual descriptions or employing a coarse-to-fine pipeline to create detailed 3D textured meshes. CLIP-Mesh [63] introduced

a novel method for zero-shot 3D model generation solely from textual prompts, achieving impressive results without the need for 3D supervision. AvatarCLIP [22] introduced a text-driven framework for 3D avatar generation and animation, utilizing CLIP [44] to enable layman users to customize avatars and animate them using natural language descriptions. Fantasia3D [9] introduces a novel method for high-quality text-to-3D content creation, emphasizing disentangled modeling of geometry and appearance, which outperforms existing methods in various task settings. DreamFusion [59] introduces a novel method leveraging a pretrained 2D text-to-image diffusion model for text-to-3D synthesis, achieving impressive results without the need for large-scale 3D datasets or modifications to the image diffusion model. ZeroAvatar [59] introduces a method for improving optimization-based image-to-3D avatar generation by incorporating an explicit 3D human body prior, resulting in enhanced robustness and 3D consistency compared to existing zero-shot methods. NIA [26] proposes a method for synthesizing varied views and poses of humans from sparse multi-view images, outperforming existing methods in both identity and pose generalization. DreamAvatar [5] proposed a text-and-shape guided framework, achieving superior performance in generating high-quality 3D human avatars with controllable poses. XAGen [60] proposed a novel method for 3D human avatar generation with expressive control over body, face, and hands, surpassing existing state-of-the-art methods in realism, diversity, and control abilities.

Recently, there’s been a promising trend in 3D generation solely from a single image, exemplified by works like Magic123 [40], Zero123 [50, 48], One-2-3-45 [28, 29], and LRM [23]. The most commonly used approach for single-image-to-3D conversion is based on the LRM paradigm, which employs an image-to-triplane decoder along with a triplane NeRF [8] or Gaussian Splatting [24] technique. Notable examples include TripoSR [54], CRM [58], TriplaneGaussian [59], and LGM [51].

**LLM-powered Agent** LLM agents utilize large language models as a central component to simulate human-like decision-making processes, playing a crucial role in the progression towards artificial general intelligence. Generative Agents [56] introduced a method to simulate believable human behavior, showcasing it in an interactive sandbox environment where agents autonomously plan and engage in social interactions. Voyager [57] introduced as the first LLM-powered embodied lifelong learning agent in Minecraft, achieving exceptional proficiency in exploration, skill acquisition, and novel discovery without human intervention. LLM-Planner [49] introduced a novel approach to few-shot planning for embodied agents, achieving competitive performance with minimal training data, thus enabling the development of versatile and sample-efficient agents capable of completing complex tasks. ELLM [13] introduced a method that leverages language model pretraining to reward agents for achieving goals suggested by a language model prompted with a description of the agent’s current state, which typically improves performance on downstream tasks. GLAM [7] introduced functional grounding to align large language models with the environment, achieving improved decision-making capabilities.

### 3 Datasets

**Zoo-300K and ZooGen** Presently, a major obstacle in generating animal motion is the lack of sufficient data pairs containing both animal motion and text descriptions. Compared to generating human motion, generating animal motion based on text commands hasn’t been explored as extensively, mostly because there’s a scarcity of suitable datasets. Animal motion datasets in research are severely limited and nowhere near as extensive as those avail-

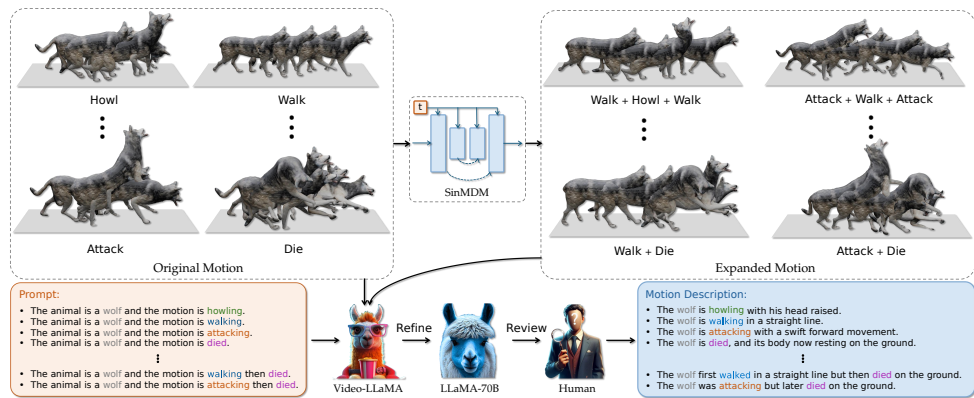


Figure 1: The diagram illustrates the process of our proposed **ZooGen**. Initially, SinMDM [40] is employed to edit and enhance motion within Truebones Zoo [2]. Subsequently, Video-LLaMA [63] is utilized to describe the motion in a paragraph, followed by refinement using LLaMA-70B [65]. Finally, human review is conducted on the motion captions, which are then gathered as textual descriptions in the **Zoo-300K** dataset.

able for human motion. To address this gap, we introduced **Zoo-300K**, a dataset containing around **300,000** pairs of text descriptions and corresponding animal motions spanning **65** different animal categories. Based on the Truebones Zoo [2] dataset, which comprises human-cultivated animal motion data annotated with textual labels denoting animal and motion categories, we have introduced a dataset construction pipeline named **ZooGen**, which facilitates the creation of a text-driven animal motion dataset, shown in fig. 1.

ZooGen utilizes SinMDM [40] to enhance motion editing and expansion capabilities, which is training a motion diffusion model on a single motion. This model can then be applied for editing and combining with other motions effectively. First, we utilize the animal motions in Truebones Zoo [2], which are cultivated by humans. For each motion, we train a unique diffusion model. These models are then used to modify other animal motions in various permutations and combinations, enabling us to acquire all the animal motions in our dataset, as shown in the upper section of fig. 1.

While human motion captioning has made strides [49, 45], accurately captioning animal motion remains a significant challenge. To address this gap, we employed a multimodal large language model Video-LLaMA [63], specifically designed for comprehensive video understanding, to describe our refined motion data. To improve the clarity and quality of captions, we use LLaMA-70B [65] for additional refinement. Eventually, these captions will undergo manual review and be selected for inclusion in the final text of Zoo-300K, as shown in the latter section of fig. 1.

**HumanML3D** For human motion generation, we used the go-to dataset HumanML3D [18], which combines 14,616 motions collected from the AMASS [60] and HumanAct12 [17] datasets. Each motion in the dataset is described by three text descriptions, totaling 44,970 scripts. It covers various actions like exercising, dancing, and acrobatics, providing a diverse collection of motion with associated language descriptions.

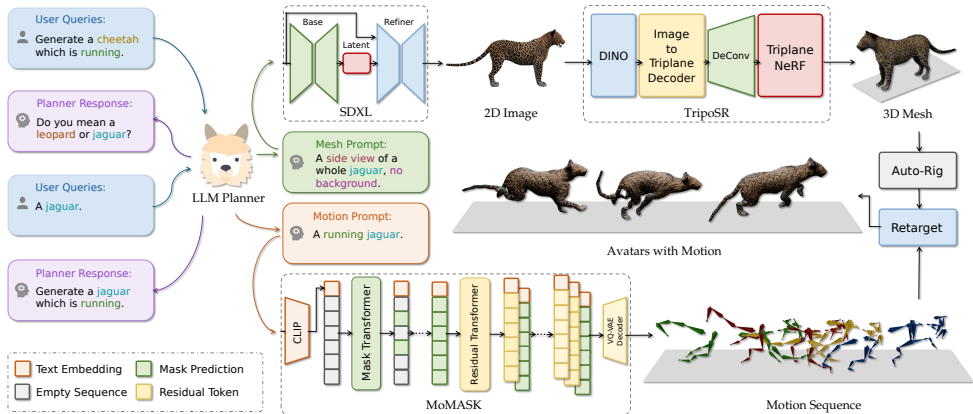


Figure 2: **Motion Avatar** utilizes a LLM-agent based approach to manage user queries and produce tailored prompts. These prompts are designed to facilitate both the generation of motion sequences and the creation of 3D meshes. Motion generation follows an autoregressive process, while mesh generation operates within an image-to-3D framework. Subsequently, the generated mesh undergoes an automatic rigging process, allowing the motion to be retargeted to the rigging mesh.

**Avatar Q&A Dataset** For tuning and evaluating our LLM planner, we’ve created the avatar Q&A dataset. This dataset utilizes animal and motion categories from Zoo-300K as input and is generated by LLaMA-70B [53]. It serves as a corpus for adjusting our LLM planner, with the *instruction* attribute used as prompts and the *output* attribute as the desired output. The dataset contains 1756 items, and Listing 1 in Appendix C provides several examples. The dataset will assess whether the LLM planner can accurately identify animal and motion categories from natural language descriptions provided by users.

## 4 Methodology

**LLM Planner** The objective of LLM planner design is to efficiently and automatically extract useful information from the user prompt  $Q_U$ , then use external components to create customizable animated avatars effectively. To efficiently deploy the planner on a local device, we developed the LLM planner leveraging the LLaMA-7B framework [53]. This planner was finely tuned using the avatar Q&A dataset to better suit the task of generating motion avatars.

In contrast to traditional text classification tasks that focus on classifying semantics within specific domains, we’ve developed our planner through instruction tuning. This approach effectively adapts the planner to our needs and activates the potential of large language model to identify motion  $M$  and avatar  $A$  categories within the dialogue between the user and the planner. Furthermore, the LLM planner possesses the ability to generate corresponding prompt  $Q_M$  and  $Q_A$  for downstream avatar motion and mesh generation, which can be formulated as:

$$(Q_M, Q_A) = \text{LLM-Planner}(Q_U) \quad (1)$$

Eventually, the LLM planner will be able to recognize main subjects in the dialogue beyond avatars and motion categories within Zoo-300K. The domain generalization capability

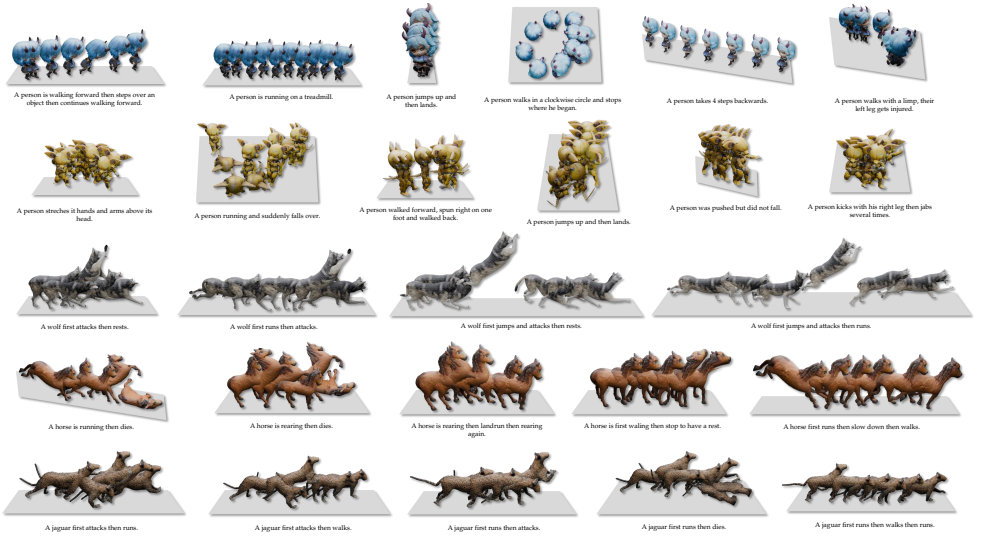


Figure 3: The figure illustrates various examples of animal motion generated by Motion Avatar, demonstrating its ability to produce high-quality motion and mesh for both human and animal characters.

of our LLM planner will help adapt to more generalizable animal motion generation tasks for the future. Meanwhile, the LLM planner effectively coordinates the avatar and motion generation components to generate personalized results that meet the users' needs, as shown in fig. 2.

**Motion Generation** Motion generation with MoMask [20] involves a two-stage training process. Firstly, a residual VQ-VAE compresses a motion sequence  $\mathbf{m}_{1:N} \in \mathbb{R}^{N \times D}$  into a latent vector  $\tilde{\mathbf{b}}_{1:n} \in \mathbb{R}^{n \times d}$ , which is then replaced with its nearest code entry in a codebook  $C = \{\mathbf{c}_k\}_{k=1}^K \subset \mathbb{R}^d$ . Then the decoder projects the quantized code sequence  $\mathbf{b}_{1:n} = Q(\tilde{\mathbf{b}}_{1:n}) \in \mathbb{R}^{n \times d}$  back to motion space for motion reconstruction  $\hat{\mathbf{m}} = D(\mathbf{b})$ .

In the second stage, both the mask transformer and the residual transformer are trained simultaneously. The text embedding  $c$  is extracted from prompt  $Q_M$  using CLIP [44], and the mask transformer draws inspiration from the bidirectional mask mechanism found in BERT [10]. Initially, the mask transformer randomly replaced a varying portion of sequence elements  $t_{1:n}^0 \in \mathbb{R}^n$  with a special [MASK] token, aiming to predict these masked tokens based on text embedding  $c$  and sequence after masking  $t^0$ . Meanwhile, the residual transformer is trained to model tokens from other  $V$  residual quantization layers. During training, a quantizer layer  $j \in [1, V]$  is randomly selected, and all tokens in the preceding layers  $t^{0:j-1}$  are embedded and summed up as the token embedding input. Using token embedding, text embedding, and the RQ layer indicator  $j$  as input, the residual transformer  $p_\phi$  is trained to predict the  $j$ -th layer tokens simultaneously.

During inference, the mask transformer is given an empty motion sequence  $t^0(0)$  as an input, and expected to generate the base-layer token sequence  $t^0$  of length  $n$  in  $L$  iterations. Then the residual transformer progressively predicts the token sequence in the rest quantiza-

tion layers. Eventually, the latent motion embedding will be decoded and projected back to motion space through the decoder of residual VQ-VAE, as shown in fig. 2.

**Avatar Generation** For generation of avatar meshes, the Motion Avatar initially employed Stable Diffusion XL [68] to utilize the mesh prompt  $Q_A$  generated by LLM planner, producing a 2D image  $I_A$  of the avatar’s front or side view tailored to requirements. The process could be described as

$$I_A = \text{SDXL}(Q_A) \quad (2)$$

Given a 2D input  $I_A$ , TripoSR [64] initially obtains the image representation using a DINO [6, 65] encoder, followed by the image-to-triplane decoder that transforms the image embedding into the triplane-NeRF [8] representation. This decoder comprises transformer layers, each featuring a self-attention layer for attending to different parts of the triplane representation and learning their relationships, and a cross-attention layer for incorporating global and local image features into the triplane representation. The triplane-NeRF [8] representation serves as a compact and expressive 3D representation, ideal for depicting objects with intricate shapes and textures. Finally, the NeRF [42] model consists of a stack of MLPs [47], responsible for predicting the color and density of a 3D point in space and rendering into a 3D mesh. The avatar mesh will be later rigged by Auto-Rig [10], enabling the motion to be retargeted to the rigged mesh, as shown in fig. 2.

## 5 Experiments

### 5.1 LLM Planner Evaluation

We extensively evaluate our LLM planner using instruction tuning on the Avatar Q&A Dataset, compared with zero-shot LLaMA-7B [63]. The results in the table 1 demonstrate that our LLM planner successfully recognizes motion and avatar categories within the dialogue between the user and the planner, showing promising potential for generalization ability in coordinating various dynamic avatar tasks. This thorough evaluation underscores the robustness and versatility of our approach in the context of dynamic avatar generation.

Models	Animal Acc. $\uparrow$	Motion Acc. $\uparrow$	Overall Acc. $\uparrow$
LLaMA-7B [63]	69.30	19.19	44.24
<b>LLM Planner (Ours)</b>	<b>97.07</b> <i>+27.77</i>	<b>71.67</b> <i>+52.48</i>	<b>84.37</b> <i>+40.13</i>

Table 1: Evaluation of our **LLM Planner** against zero-shot LLaMA-7B [63] on the Avatar Q&A Dataset reveals its successful recognition of motion and avatar categories during user-planner dialogue.

### 5.2 Motion Evaluation

Since human motion generation has already been evaluated in the MoMask [20], our focus shifts to comprehensively assessing animal motion generation utilizing the newly introduced Zoo-300K dataset. For quantitative results, please refer to the table in **Appendix A: Animal Motion Quantative Evaluation** and **Appendix B: User Study** in supplementary. For qualitative assessment, the visualization in fig. 3 illustrates our model’s capability to seamlessly generate animal motion based on text conditions, showcasing potential applications in fields like computer gaming and film making. These findings highlight the versatility and effectiveness of our approach in diverse scenarios.

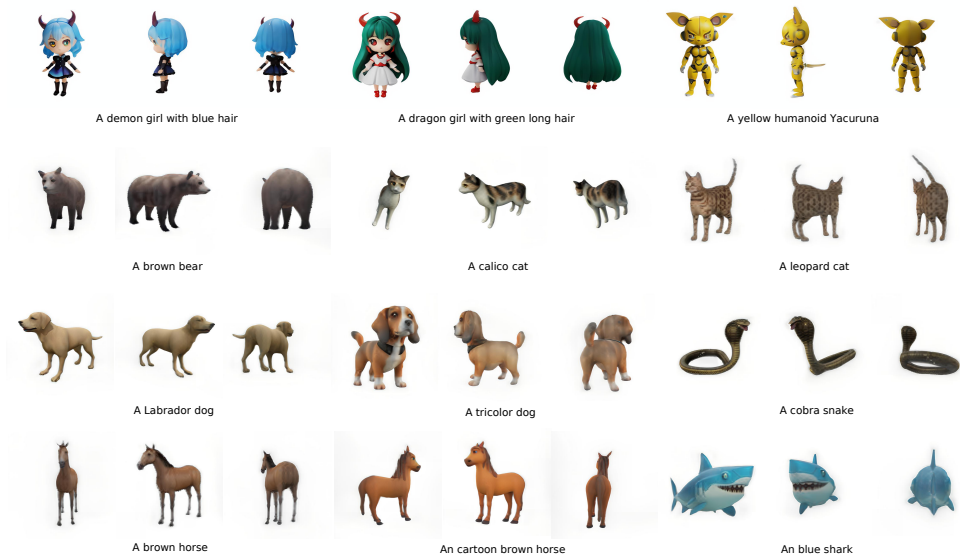


Figure 4: The figure showcases various examples of generated 3D meshes, encompassing both human and animal avatars. The meshes exhibit high-quality geometry and offer customizable textures, thus serving as a robust foundation for avatar animation. Furthermore, this advancement holds promise for enhancing the technique’s applicability in real-world scenarios.

### 5.3 Avatar Evaluation

Given that TripoSR [64] has already conducted quantitative evaluations for 3D mesh generation, we extended our evaluation to generating 3D avatars using the character categories in the Zoo-300K dataset to assess our model’s adaptation to our task. The fig. 4 illustrates randomly selected examples of 3D avatars generated by our model. The results demonstrate that our model can produce high-quality and detailed 3D avatars, indicating its utility for avatar motion generation.

## 6 Discussion and Conclusion

In conclusion, our study addresses the ongoing challenges in dynamic 3D avatar generation by presenting innovative solutions. Through the introduction of Motion Avatar, a novel agent-based approach, we enable the automatic creation of highly customizable human and animal avatars complete with dynamic motions based on text queries, thus advancing the field significantly. Additionally, our LLM planner facilitates the coordination of motion and avatar generation, enhancing adaptability and usability in dynamic avatar tasks. Furthermore, the development of the Zoo-300K dataset, alongside the ZooGen pipeline, provides a valuable resource for researchers, underscoring our commitment to advancing the field of dynamic avatar generation across various domains.

## References

- [1] Auto-rig pro. URL <https://blendermarket.com/products/auto-rig-pro>.
- [2] Free fbx/bvh zoo. animals with animations and textures. URL <https://truebones.gumroad.com/l/skZMC>.
- [3] Josh Achiam, Steven Adler, Sandhini Agarwal, Lama Ahmad, Ilge Akkaya, Florencia Leoni Aleman, Diogo Almeida, Janko Altenschmidt, Sam Altman, Shyamal Anadkat, et al. Gpt-4 technical report. *arXiv preprint arXiv:2303.08774*, 2023.
- [4] Tom Brown, Benjamin Mann, Nick Ryder, Melanie Subbiah, Jared D Kaplan, Prafulla Dhariwal, Arvind Neelakantan, Pranav Shyam, Girish Sastry, Amanda Askell, et al. Language models are few-shot learners. *Advances in neural information processing systems*, 33:1877–1901, 2020.
- [5] Yukang Cao, Yan-Pei Cao, Kai Han, Ying Shan, and Kwan-Yee K Wong. Dreamavatar: Text-and-shape guided 3d human avatar generation via diffusion models. *arXiv preprint arXiv:2304.00916*, 2023.
- [6] Mathilde Caron, Hugo Touvron, Ishan Misra, Hervé Jégou, Julien Mairal, Piotr Bojanowski, and Armand Joulin. Emerging properties in self-supervised vision transformers. In *Proceedings of the IEEE/CVF international conference on computer vision*, pages 9650–9660, 2021.
- [7] Thomas Carta, Clément Romac, Thomas Wolf, Sylvain Lamprier, Olivier Sigaud, and Pierre-Yves Oudeyer. Grounding large language models in interactive environments with online reinforcement learning. In *International Conference on Machine Learning*, pages 3676–3713. PMLR, 2023.
- [8] Eric R Chan, Connor Z Lin, Matthew A Chan, Koki Nagano, Boxiao Pan, Shalini De Mello, Orazio Gallo, Leonidas J Guibas, Jonathan Tremblay, Sameh Khamis, et al. Efficient geometry-aware 3d generative adversarial networks. In *Proceedings of the IEEE/CVF conference on computer vision and pattern recognition*, pages 16123–16133, 2022.
- [9] Rui Chen, Yongwei Chen, Ningxin Jiao, and Kui Jia. Fantasia3d: Disentangling geometry and appearance for high-quality text-to-3d content creation. In *Proceedings of the IEEE/CVF International Conference on Computer Vision*, pages 22246–22256, 2023.
- [10] Xin Chen, Biao Jiang, Wen Liu, Zilong Huang, Bin Fu, Tao Chen, and Gang Yu. Executing your commands via motion diffusion in latent space. In *Proceedings of the IEEE/CVF Conference on Computer Vision and Pattern Recognition*, pages 18000–18010, 2023.
- [11] Jacob Devlin, Ming-Wei Chang, Kenton Lee, and Kristina Toutanova. Bert: Pre-training of deep bidirectional transformers for language understanding. *arXiv preprint arXiv:1810.04805*, 2018.
- [12] Prafulla Dhariwal and Alexander Nichol. Diffusion models beat gans on image synthesis. *Advances in neural information processing systems*, 34:8780–8794, 2021.

- [13] Yuqing Du, Olivia Watkins, Zihan Wang, Cédric Colas, Trevor Darrell, Pieter Abbeel, Abhishek Gupta, and Jacob Andreas. Guiding pretraining in reinforcement learning with large language models. In *International Conference on Machine Learning*, pages 8657–8677. PMLR, 2023.
- [14] Quankai Gao, Qiangeng Xu, Zhe Cao, Ben Mildenhall, Wenchao Ma, Le Chen, Danhang Tang, and Ulrich Neumann. Gaussianflow: Splatting gaussian dynamics for 4d content creation. *arXiv preprint arXiv:2403.12365*, 2024.
- [15] Kehong Gong, Dongze Lian, Heng Chang, Chuan Guo, Zihang Jiang, Xinxin Zuo, Michael Bi Mi, and Xinchao Wang. Tm2d: Bimodality driven 3d dance generation via music-text integration. In *Proceedings of the IEEE/CVF International Conference on Computer Vision*, pages 9942–9952, 2023.
- [16] Albert Gu and Tri Dao. Mamba: Linear-time sequence modeling with selective state spaces. *arXiv preprint arXiv:2312.00752*, 2023.
- [17] Chuan Guo, Xinxin Zuo, Sen Wang, Shihao Zou, Qingyao Sun, Annan Deng, Minglun Gong, and Li Cheng. Action2motion: Conditioned generation of 3d human motions. In *Proceedings of the 28th ACM International Conference on Multimedia*, pages 2021–2029, 2020.
- [18] Chuan Guo, Shihao Zou, Xinxin Zuo, Sen Wang, Wei Ji, Xingyu Li, and Li Cheng. Generating diverse and natural 3d human motions from text. In *Proceedings of the IEEE/CVF Conference on Computer Vision and Pattern Recognition*, pages 5152–5161, 2022.
- [19] Chuan Guo, Xinxin Zuo, Sen Wang, and Li Cheng. Tm2t: Stochastic and tokenized modeling for the reciprocal generation of 3d human motions and texts. In *European Conference on Computer Vision*, pages 580–597. Springer, 2022.
- [20] Chuan Guo, Yuxuan Mu, Muhammad Gohar Javed, Sen Wang, and Li Cheng. Momask: Generative masked modeling of 3d human motions. *arXiv preprint arXiv:2312.00063*, 2023.
- [21] Jonathan Ho, Ajay Jain, and Pieter Abbeel. Denoising diffusion probabilistic models. *Advances in neural information processing systems*, 33:6840–6851, 2020.
- [22] Fangzhou Hong, Mingyuan Zhang, Liang Pan, Zhongang Cai, Lei Yang, and Ziwei Liu. Avatarclip: Zero-shot text-driven generation and animation of 3d avatars. *arXiv preprint arXiv:2205.08535*, 2022.
- [23] Yicong Hong, Kai Zhang, Jiuxiang Gu, Sai Bi, Yang Zhou, Difan Liu, Feng Liu, Kalyan Sunkavalli, Trung Bui, and Hao Tan. Lrm: Large reconstruction model for single image to 3d. In *The Twelfth International Conference on Learning Representations*, 2023.
- [24] Bernhard Kerbl, Georgios Kopanas, Thomas Leimkühler, and George Drettakis. 3d gaussian splatting for real-time radiance field rendering. *ACM Transactions on Graphics*, 42(4):1–14, 2023.
- [25] Diederik P Kingma and Max Welling. Auto-encoding variational bayes. *arXiv preprint arXiv:1312.6114*, 2013.

- [26] YoungJoong Kwon, Dahun Kim, Duygu Ceylan, and Henry Fuchs. Neural image-based avatars: Generalizable radiance fields for human avatar modeling. In *The Eleventh International Conference on Learning Representations*, 2022.
- [27] Isabella Liu, Hao Su, and Xiaolong Wang. Dynamic gaussians mesh: Consistent mesh reconstruction from monocular videos. *arXiv preprint arXiv:2404.12379*, 2024.
- [28] Minghua Liu, Ruoxi Shi, Linghao Chen, Zhuoyang Zhang, Chao Xu, Xinyue Wei, Hansheng Chen, Chong Zeng, Jiayuan Gu, and Hao Su. One-2-3-45++: Fast single image to 3d objects with consistent multi-view generation and 3d diffusion. *arXiv preprint arXiv:2311.07885*, 2023.
- [29] Minghua Liu, Chao Xu, Haian Jin, Linghao Chen, Mukund Varma T, Zexiang Xu, and Hao Su. One-2-3-45: Any single image to 3d mesh in 45 seconds without per-shape optimization. *Advances in Neural Information Processing Systems*, 36, 2024.
- [30] Ruoshi Liu, Rundi Wu, Basile Van Hoorick, Pavel Tokmakov, Sergey Zakharov, and Carl Vondrick. Zero-1-to-3: Zero-shot one image to 3d object. In *Proceedings of the IEEE/CVF International Conference on Computer Vision*, pages 9298–9309, 2023.
- [31] Naureen Mahmood, Nima Ghorbani, Nikolaus F Troje, Gerard Pons-Moll, and Michael J Black. Amass: Archive of motion capture as surface shapes. In *Proceedings of the IEEE/CVF international conference on computer vision*, pages 5442–5451, 2019.
- [32] Ben Mildenhall, Pratul P Srinivasan, Matthew Tancik, Jonathan T Barron, Ravi Ramamoorthi, and Ren Ng. Nerf: Representing scenes as neural radiance fields for view synthesis. *Communications of the ACM*, 65(1):99–106, 2021.
- [33] Nasir Mohammad Khalid, Tianhao Xie, Eugene Belilovsky, and Tiberiu Popa. Clip-mesh: Generating textured meshes from text using pretrained image-text models. In *SIGGRAPH Asia 2022 conference papers*, pages 1–8, 2022.
- [34] Alex Nichol, Prafulla Dhariwal, Aditya Ramesh, Pranav Shyam, Pamela Mishkin, Bob McGrew, Ilya Sutskever, and Mark Chen. Glide: Towards photorealistic image generation and editing with text-guided diffusion models. *arXiv preprint arXiv:2112.10741*, 2021.
- [35] Maxime Oquab, Timothée Darcet, Théo Moutakanni, Huy Vo, Marc Szafraniec, Vasil Khalidov, Pierre Fernandez, Daniel Haziza, Francisco Massa, Alaaeldin El-Nouby, et al. Dinov2: Learning robust visual features without supervision. *arXiv preprint arXiv:2304.07193*, 2023.
- [36] Joon Sung Park, Joseph O’Brien, Carrie Jun Cai, Meredith Ringel Morris, Percy Liang, and Michael S Bernstein. Generative agents: Interactive simulacra of human behavior. In *Proceedings of the 36th Annual ACM Symposium on User Interface Software and Technology*, pages 1–22, 2023.
- [37] Mathis Petrovich, Michael J Black, and Gül Varol. Temos: Generating diverse human motions from textual descriptions. In *European Conference on Computer Vision*, pages 480–497. Springer, 2022.

- [38] Dustin Podell, Zion English, Kyle Lacey, Andreas Blattmann, Tim Dockhorn, Jonas Müller, Joe Penna, and Robin Rombach. Sdxl: Improving latent diffusion models for high-resolution image synthesis. *arXiv preprint arXiv:2307.01952*, 2023.
- [39] Ben Poole, Ajay Jain, Jonathan T Barron, and Ben Mildenhall. Dreamfusion: Text-to-3d using 2d diffusion. *arXiv preprint arXiv:2209.14988*, 2022.
- [40] Guocheng Qian, Jinjie Mai, Abdullah Hamdi, Jian Ren, Aliaksandr Siarohin, Bing Li, Hsin-Ying Lee, Ivan Skorokhodov, Peter Wonka, Sergey Tulyakov, et al. Magic123: One image to high-quality 3d object generation using both 2d and 3d diffusion priors. *arXiv preprint arXiv:2306.17843*, 2023.
- [41] Sigal Raab, Inbal Leibovitch, Guy Tevet, Moab Arar, Amit Haim Bermano, and Daniel Cohen-Or. Single motion diffusion. In *The Twelfth International Conference on Learning Representations*, 2023.
- [42] Alec Radford, Karthik Narasimhan, Tim Salimans, Ilya Sutskever, et al. Improving language understanding by generative pre-training. 2018.
- [43] Alec Radford, Jeffrey Wu, Rewon Child, David Luan, Dario Amodei, Ilya Sutskever, et al. Language models are unsupervised multitask learners. *OpenAI blog*, 1(8):9, 2019.
- [44] Alec Radford, Jong Wook Kim, Chris Hallacy, Aditya Ramesh, Gabriel Goh, Sandhini Agarwal, Girish Sastry, Amanda Askell, Pamela Mishkin, Jack Clark, et al. Learning transferable visual models from natural language supervision. In *International conference on machine learning*, pages 8748–8763. PMLR, 2021.
- [45] Karim Radouane, Andon Tchechmedjiev, Julien Lagarde, and Sylvie Ranwez. Motion2language, unsupervised learning of synchronized semantic motion segmentation. *Neural Computing and Applications*, 36(8):4401–4420, 2024.
- [46] Robin Rombach, Andreas Blattmann, Dominik Lorenz, Patrick Esser, and Björn Ommer. High-resolution image synthesis with latent diffusion models. In *Proceedings of the IEEE/CVF conference on computer vision and pattern recognition*, pages 10684–10695, 2022.
- [47] David E Rumelhart, Geoffrey E Hinton, and Ronald J Williams. Learning internal representations by error propagation, parallel distributed processing, explorations in the microstructure of cognition, ed. de rumelhart and j. mcclelland. vol. 1. 1986. *Biometrika*, 71:599–607, 1986.
- [48] Ruoxi Shi, Hansheng Chen, Zhuoyang Zhang, Minghua Liu, Chao Xu, Xinyue Wei, Linghao Chen, Chong Zeng, and Hao Su. Zero123++: a single image to consistent multi-view diffusion base model. *arXiv preprint arXiv:2310.15110*, 2023.
- [49] Chan Hee Song, Jiaman Wu, Clayton Washington, Brian M Sadler, Wei-Lun Chao, and Yu Su. Llm-planner: Few-shot grounded planning for embodied agents with large language models. In *Proceedings of the IEEE/CVF International Conference on Computer Vision*, pages 2998–3009, 2023.
- [50] Jiaming Song, Chenlin Meng, and Stefano Ermon. Denoising diffusion implicit models. In *International Conference on Learning Representations*, 2020.

- [51] Jiayang Tang, Zhaoxi Chen, Xiaokang Chen, Tengfei Wang, Gang Zeng, and Ziwei Liu. Lgm: Large multi-view gaussian model for high-resolution 3d content creation. *arXiv preprint arXiv:2402.05054*, 2024.
- [52] Guy Tevet, Brian Gordon, Amir Hertz, Amit H Bermano, and Daniel Cohen-Or. Motionclip: Exposing human motion generation to clip space. In *European Conference on Computer Vision*, pages 358–374. Springer, 2022.
- [53] Guy Tevet, Sigal Raab, Brian Gordon, Yoni Shafir, Daniel Cohen-or, and Amit Haim Bermano. Human motion diffusion model. In *The Eleventh International Conference on Learning Representations*, 2022.
- [54] Dmitry Tochilkin, David Pankratz, Zexiang Liu, Zixuan Huang, Adam Letts, Yangguang Li, Ding Liang, Christian Laforte, Varun Jampani, and Yan-Pei Cao. Triposr: Fast 3d object reconstruction from a single image. *arXiv preprint arXiv:2403.02151*, 2024.
- [55] Hugo Touvron, Thibaut Lavril, Gautier Izacard, Xavier Martinet, Marie-Anne Lachaux, Timothée Lacroix, Baptiste Rozière, Naman Goyal, Eric Hambro, Faisal Azhar, et al. Llama: Open and efficient foundation language models. *arXiv preprint arXiv:2302.13971*, 2023.
- [56] Ashish Vaswani, Noam Shazeer, Niki Parmar, Jakob Uszkoreit, Llion Jones, Aidan N Gomez, Łukasz Kaiser, and Illia Polosukhin. Attention is all you need. *Advances in neural information processing systems*, 30, 2017.
- [57] Guanzhi Wang, Yuqi Xie, Yunfan Jiang, Ajay Mandlekar, Chaowei Xiao, Yuke Zhu, Linxi Fan, and Anima Anandkumar. Voyager: An open-ended embodied agent with large language models. *arXiv preprint arXiv:2305.16291*, 2023.
- [58] Zhengyi Wang, Yikai Wang, Yifei Chen, Chendong Xiang, Shuo Chen, Dajiang Yu, Chongxuan Li, Hang Su, and Jun Zhu. Crm: Single image to 3d textured mesh with convolutional reconstruction model. *arXiv preprint arXiv:2403.05034*, 2024.
- [59] Zhenzhen Weng, Zeyu Wang, and Serena Yeung. Zeroavatar: Zero-shot 3d avatar generation from a single image. *arXiv preprint arXiv:2305.16411*, 2023.
- [60] Zhongcong Xu, Jianfeng Zhang, Jun Hao Liew, Jiashi Feng, and Mike Zheng Shou. Xagen: 3d expressive human avatars generation. *Advances in Neural Information Processing Systems*, 36, 2024.
- [61] Zhangsihao Yang, Mingyuan Zhou, Mengyi Shan, Bingbing Wen, Ziwei Xuan, Mitch Hill, Junjie Bai, Guo-Jun Qi, and Yalin Wang. Omnimotiongpt: Animal motion generation with limited data. *arXiv preprint arXiv:2311.18303*, 2023.
- [62] Yuyang Yin, Dejia Xu, Zhangyang Wang, Yao Zhao, and Yunchao Wei. 4dgen: Grounded 4d content generation with spatial-temporal consistency. *arXiv preprint arXiv:2312.17225*, 2023.
- [63] Hang Zhang, Xin Li, and Lidong Bing. Video-llama: An instruction-tuned audio-visual language model for video understanding. In *Proceedings of the 2023 Conference on Empirical Methods in Natural Language Processing: System Demonstrations*, pages 543–553, 2023.

- [64] Mingyuan Zhang, Zhongang Cai, Liang Pan, Fangzhou Hong, Xinying Guo, Lei Yang, and Ziwei Liu. Motiondiffuse: Text-driven human motion generation with diffusion model. *IEEE Transactions on Pattern Analysis and Machine Intelligence*, 2024.
- [65] Zeyu Zhang, Akide Liu, Qi Chen, Feng Chen, Ian Reid, Richard Hartley, Bohan Zhuang, and Hao Tang. Infinimotion: Mamba boosts memory in transformer for arbitrary long motion generation. *arXiv preprint arXiv:2407.10061*, 2024.
- [66] Zeyu Zhang, Akide Liu, Ian Reid, Richard Hartley, Bohan Zhuang, and Hao Tang. Motion mamba: Efficient and long sequence motion generation with hierarchical and bidirectional selective ssm. *arXiv preprint arXiv:2403.07487*, 2024.
- [67] Yuyang Zhao, Zhiwen Yan, Enze Xie, Lanqing Hong, Zhenguo Li, and Gim Hee Lee. Animate124: Animating one image to 4d dynamic scene. *arXiv preprint arXiv:2311.14603*, 2023.
- [68] Chongyang Zhong, Lei Hu, Zihao Zhang, and Shihong Xia. Att2m: Text-driven human motion generation with multi-perspective attention mechanism. In *Proceedings of the IEEE/CVF International Conference on Computer Vision*, pages 509–519, 2023.
- [69] Zi-Xin Zou, Zhipeng Yu, Yuan-Chen Guo, Yangguang Li, Ding Liang, Yan-Pei Cao, and Song-Hai Zhang. Triplane meets gaussian splatting: Fast and generalizable single-view 3d reconstruction with transformers. *arXiv preprint arXiv:2312.09147*, 2023.

## Appendix

### A Animal Motion Quantative Evaluation

We evaluated our Motion Avatar on the Zoo-300K dataset, and the results are presented in table 2. The comprehensive evaluation demonstrated that our method achieves high-quality animal motion generation. The results indicate that our approach produces highly realistic and promising animations, highlighting the effectiveness and potential of our technique in generating detailed and lifelike animal motions.

### B User Study

In this work, we conduct an exhaustive evaluation of the effectiveness of our motion avatar generation, leveraging both qualitative and quantitative assessments. This user study assesses the real-world applicability of 4 motion video generated from the Motion Avatar platform by the input prompt, examined by 50 participants through a Google Forms interface as in Fig 5.

Participants were presented with four videos labeled Video A, Video B, Video C, and Video D. Each video showcased a unique motion generated using Motion Avatar with different input prompt. The participants evaluated these videos by responding to a series of targeted questions aimed at assessing the motion’s accuracy, the mesh’s visual quality, the integration of motion and mesh, and their overall emotional response to the animations.

The evaluation was structured around several key aspects:

1. **Motion Accuracy:** Participants rated the naturalness and accuracy of the motions on a scale from 1 (‘Very Inaccurate’) to 5 (‘Very Natural’). The average score was 4.2, indicating a high fidelity in motion portrayal.
2. **Mesh Quality:** The visual quality and detail of the mesh were rated from 1 (‘Poor Quality’) to 5 (‘Excellent Quality’), with an average score of 4.0, highlighting the superior visual appeal of our models.
3. **Motion and Mesh Integration:** The integration of motion and mesh was assessed, with most participants rating this aspect a 4.5 on average, reflecting seamless integration that enhances fluidity and realism.
4. **User Engagement and Appeal:** Participants reflected on their feelings towards the animations, rating their overall engagement and appeal from 1 (‘Not Engaging’) to 5 (‘Highly Engaging’). The average engagement score was 4.3, suggesting that the animations were highly engaging and appealing to the audience.

Results suggested that:

- 92% of participants believed the animations could be directly utilized in real-world applications without significant modifications.
- Only 8% felt that minor adjustments were necessary before deployment.

These findings underscore the high quality, impressive results, and broad usability of the animations. Nearly all participants found the quality of the generated videos to be very high,

Table 2: The table shows that our **Motion Avatar** achieves high-quality animal motion generation on the Zoo-300K dataset. It demonstrates the effectiveness of our method, producing realistic and promising animal motions.

Method	R-Prec Top 1 $\uparrow$	R-Prec Top 2 $\uparrow$	R-Prec Top 3 $\uparrow$	FID $\downarrow$	MultiModal-Dist $\downarrow$	Diversity $\rightarrow$
Anaconda (GT)	0.400	0.591	0.713	0.015	2.870	10.233
<b>Anaconda (Ours)</b>	<b>0.042</b>	<b>0.080</b>	<b>0.128</b>	<b>0.51067</b>	<b>9.053</b>	<b>5.165</b>
Ant (GT)	0.413	0.650	0.768	0.12	2.000	9.700
<b>Ant (Ours)</b>	<b>0.056</b>	<b>0.110</b>	<b>0.166</b>	<b>68.220</b>	<b>9.380</b>	<b>4.380</b>
Bat (GT)	0.406	0.677	0.841	0.011	1.805	12.084
<b>Bat (Ours)</b>	<b>0.193</b>	<b>0.536</b>	<b>0.086</b>	<b>79.403</b>	<b>9.430</b>	<b>0.984</b>
Bear (GT)	0.641	0.851	0.916	0.012	1.827	13.587
<b>Bear (Ours)</b>	<b>0.156</b>	<b>0.287</b>	<b>0.382</b>	<b>35.735</b>	<b>8.890</b>	<b>4.364</b>
Bird (GT)	0.569	0.762	0.851	0.004	2.679	12.294
<b>Bird (Ours)</b>	<b>0.059</b>	<b>0.091</b>	<b>0.127</b>	<b>54.735</b>	<b>9.726</b>	<b>4.389</b>
Buffalo (GT)	0.547	0.750	0.852	0.014	3.876	16.405
<b>Buffalo (Ours)</b>	<b>0.070</b>	<b>0.140</b>	<b>0.227</b>	<b>167.900</b>	<b>13.378</b>	<b>4.352</b>
Buzzard (GT)	0.423	0.639	0.778	0.007	2.654	11.045
<b>Buzzard (Ours)</b>	<b>0.034</b>	<b>0.084</b>	<b>0.111</b>	<b>65.274</b>	<b>8.645</b>	<b>1.824</b>
Camel (GT)	0.297	0.469	0.609	0.014	3.381	11.025
<b>Camel (Ours)</b>	<b>0.078</b>	<b>0.188</b>	<b>0.250</b>	<b>92.963</b>	<b>11.654</b>	<b>5.249</b>
Cat (GT)	0.141	0.281	0.422	0.041	2.274	9.060
<b>Cat (Ours)</b>	<b>0.063</b>	<b>0.188</b>	<b>0.219</b>	<b>56.405</b>	<b>7.195</b>	<b>1.969</b>
Centipede (GT)	0.386	0.580	0.712	0.026	2.256	11.279
<b>Centipede (Ours)</b>	<b>0.123</b>	<b>0.223</b>	<b>0.317</b>	<b>65.076</b>	<b>8.590</b>	<b>5.664</b>
Chicken (GT)	0.094	0.203	0.313	0.075	3.503	9.196
<b>Chicken (Ours)</b>	<b>0.063</b>	<b>0.141</b>	<b>0.172</b>	<b>70.271</b>	<b>7.953</b>	<b>2.752</b>
Cobra (GT)	0.386	0.583	0.700	0.009	2.881	10.901
<b>Cobra (Ours)</b>	<b>0.217</b>	<b>0.324</b>	<b>0.406</b>	<b>0.309</b>	<b>6.397</b>	<b>10.823</b>
Komodo (GT)	0.260	0.375	0.456	0.064	5.208	9.968
<b>Komodo (Ours)</b>	<b>0.073</b>	<b>0.125</b>	<b>0.161</b>	<b>43.677</b>	<b>7.074</b>	<b>3.047</b>
Coyote (GT)	0.523	0.765	0.869	0.034	2.042	12.985
<b>Coyote (Ours)</b>	<b>0.052</b>	<b>0.102</b>	<b>0.158</b>	<b>89.865</b>	<b>9.834</b>	<b>2.396</b>
Crab (GT)	0.367	0.570	0.698	0.019	2.373	12.260
<b>Crab (Ours)</b>	<b>0.066</b>	<b>0.109</b>	<b>0.175</b>	<b>79.233</b>	<b>9.862</b>	<b>2.737</b>
Cricket (GT)	0.429	0.658	0.777	0.003	2.015	14.790
<b>Cricket (Ours)</b>	<b>0.036</b>	<b>0.075</b>	<b>0.111</b>	<b>111.337</b>	<b>12.126</b>	<b>3.810</b>
Crocodile (GT)	0.567	0.879	0.891	0.016	2.177	13.694
<b>Crocodile (Ours)</b>	<b>0.054</b>	<b>0.094</b>	<b>0.133</b>	<b>86.886</b>	<b>10.049</b>	<b>2.827</b>
Crow (GT)	0.390	0.644	0.796	0.018	2.682	12.131
<b>Crow (Ours)</b>	<b>0.034</b>	<b>0.058</b>	<b>0.079</b>	<b>61.148</b>	<b>10.915</b>	<b>5.021</b>
Deer (GT)	0.497	0.722	0.816	0.010	2.700	11.116
<b>Deer (Ours)</b>	<b>0.092</b>	<b>0.174</b>	<b>0.231</b>	<b>12.931</b>	<b>8.106</b>	<b>8.577</b>
Dog (GT)	0.609	0.850	0.940	0.025	2.001	15.927
<b>Dog (Ours)</b>	<b>0.039</b>	<b>0.086</b>	<b>0.111</b>	<b>80.711</b>	<b>12.049</b>	<b>4.249</b>
Eagle (GT)	0.551	0.788	0.896	0.003	1.607	14.266
<b>Eagle (Ours)</b>	<b>0.057</b>	<b>0.121</b>	<b>0.169</b>	<b>65.728</b>	<b>10.753</b>	<b>4.716</b>
Elephant (GT)	0.544	0.750	0.851	0.006	2.331	14.017
<b>Elephant (Ours)</b>	<b>0.044</b>	<b>0.091</b>	<b>0.136</b>	<b>91.635</b>	<b>10.651</b>	<b>2.837</b>
Fire Ant (GT)	0.399	0.587	0.692	0.004	3.602	9.441
<b>Fire Ant (Ours)</b>	<b>0.027</b>	<b>0.055</b>	<b>0.081</b>	<b>48.101</b>	<b>7.988</b>	<b>2.065</b>
Flamingo (GT)	0.078	0.250	0.375	0.023	2.971	8.589
<b>Flamingo (Ours)</b>	<b>0.031</b>	<b>0.062</b>	<b>0.109</b>	<b>47.836</b>	<b>8.396</b>	<b>3.119</b>
Fox (GT)	0.380	0.566	0.723	0.009	2.807	11.209
<b>Fox (Ours)</b>	<b>0.061</b>	<b>0.128</b>	<b>0.179</b>	<b>30.368</b>	<b>9.234</b>	<b>7.117</b>

Table 3: Continued from Table 2.

Method	R-Prec Top 1 $\uparrow$	R-Prec Top 2 $\uparrow$	R-Prec Top 3 $\uparrow$	FID $\downarrow$	MultiModal-Dist $\downarrow$	Diversity $\rightarrow$
Gazelle (GT)	0.462	0.700	0.825	0.024	2.401	12.907
<b>Gazelle (Ours)</b>	<b>0.019</b>	<b>0.041</b>	<b>0.075</b>	<b>95.267</b>	<b>11.966</b>	<b>4.100</b>
Giant Bee (GT)	0.353	0.555	0.703	0.029	2.700	12.992
<b>Giant Bee (Ours)</b>	<b>0.097</b>	<b>0.167</b>	<b>0.234</b>	<b>63.874</b>	<b>9.436</b>	<b>5.031</b>
Goat (GT)	0.394	0.663	0.825	0.013	1.975	11.550
<b>Goat (Ours)</b>	<b>0.033</b>	<b>0.064</b>	<b>0.094</b>	<b>102.515</b>	<b>10.767</b>	<b>2.069</b>
Hamster (GT)	0.297	0.531	0.672	0.039	2.251	12.088
<b>Hamster (Ours)</b>	<b>0.052</b>	<b>0.104</b>	<b>0.141</b>	<b>108.243</b>	<b>10.693</b>	<b>2.000</b>
Hermit Crab (GT)	0.439	0.680	0.811	0.009	2.677	10.232
<b>Hermit Crab (Ours)</b>	<b>0.046</b>	<b>0.085</b>	<b>0.113</b>	<b>45.140</b>	<b>8.103</b>	<b>2.704</b>
Hippopotamus (GT)	0.542	0.773	0.879	0.044	2.201	11.970
<b>Hippopotamus (Ours)</b>	<b>0.052</b>	<b>0.102</b>	<b>0.139</b>	<b>86.651</b>	<b>9.931</b>	<b>1.684</b>
Horse (GT)	0.518	0.686	0.779	0.006	2.816	10.935
<b>Horse (Ours)</b>	<b>0.053</b>	<b>0.090</b>	<b>0.137</b>	<b>31.290</b>	<b>9.131</b>	<b>6.203</b>
Hound (GT)	0.639	0.822	0.909	0.014	2.519	11.514
<b>Hound (Ours)</b>	<b>0.047</b>	<b>0.107</b>	<b>0.146</b>	<b>68.021</b>	<b>9.198</b>	<b>2.529</b>
Isopetra (GT)	0.498	0.708	0.824	0.020	2.710	11.242
<b>Isopetra (Ours)</b>	<b>0.035</b>	<b>0.088</b>	<b>0.127</b>	<b>56.617</b>	<b>9.598</b>	<b>3.903</b>
Jaguar (GT)	0.538	0.762	0.871	0.009	2.354	11.287
<b>Jaguar (Ours)</b>	<b>0.043</b>	<b>0.074</b>	<b>0.105</b>	<b>71.047</b>	<b>9.314</b>	<b>2.442</b>
Leopard (GT)	0.558	0.758	0.884	0.017	1.989	13.777
<b>Leopard (Ours)</b>	<b>0.058</b>	<b>0.115</b>	<b>0.152</b>	<b>67.369</b>	<b>9.686</b>	<b>4.035</b>
Lion (GT)	0.542	0.756	0.881	0.010	2.357	11.772
<b>Lion (Ours)</b>	<b>0.042</b>	<b>0.066</b>	<b>0.107</b>	<b>79.524</b>	<b>9.760</b>	<b>2.419</b>
Lynx (GT)	0.526	0.751	0.869	0.019	2.158	12.317
<b>Lynx (Ours)</b>	<b>0.059</b>	<b>0.096</b>	<b>0.140</b>	<b>77.358</b>	<b>9.666</b>	<b>2.858</b>
Mammoth (GT)	0.551	0.775	0.860	0.004	2.518	12.963
<b>Mammoth (Ours)</b>	<b>0.055</b>	<b>0.112</b>	<b>0.155</b>	<b>80.510</b>	<b>9.973</b>	<b>2.614</b>
Monkey (GT)	0.361	0.551	0.683	0.015	3.425	11.441
<b>Monkey (Ours)</b>	<b>0.053</b>	<b>0.082</b>	<b>0.118</b>	<b>31.473</b>	<b>8.819</b>	<b>2.880</b>
Ostrich (GT)	0.508	0.691	0.817	0.011	2.507	12.145
<b>Ostrich (Ours)</b>	<b>0.084</b>	<b>0.145</b>	<b>0.189</b>	<b>59.510</b>	<b>9.215</b>	<b>3.988</b>
Parrot (GT)	0.524	0.754	0.859	0.040	2.091	14.021
<b>Parrot (Ours)</b>	<b>0.068</b>	<b>0.149</b>	<b>0.202</b>	<b>27.881</b>	<b>10.990</b>	<b>9.306</b>
Pigeon (GT)	0.431	0.670	0.810	0.047	2.151	11.879
<b>Pigeon (Ours)</b>	<b>0.208</b>	<b>0.328</b>	<b>0.426</b>	<b>0.431</b>	<b>7.187</b>	<b>11.446</b>
Piranha (GT)	0.287	0.499	0.684	0.010	2.262	11.645
<b>Piranha (Ours)</b>	<b>0.038</b>	<b>0.069</b>	<b>0.096</b>	<b>81.586</b>	<b>9.930</b>	<b>1.719</b>
Polar Bear (GT)	0.519	0.746	0.867	0.024	2.162	12.509
<b>Polar Bear (Ours)</b>	<b>0.031</b>	<b>0.065</b>	<b>0.102</b>	<b>112.532</b>	<b>11.160</b>	<b>3.155</b>
Pteranodon (GT)	0.510	0.730	0.815	0.021	2.704	10.532
<b>Pteranodon (Ours)</b>	<b>0.037</b>	<b>0.076</b>	<b>0.121</b>	<b>26.197</b>	<b>8.329</b>	<b>1.424</b>
Puppy (GT)	0.344	0.563	0.729	0.036	1.421	12.181
<b>Puppy (Ours)</b>	<b>0.094</b>	<b>0.240</b>	<b>0.292</b>	<b>55.135</b>	<b>8.730</b>	<b>5.339</b>
Raptor (GT)	0.531	0.781	0.881	0.066	1.896	13.216
<b>Raptor (Ours)</b>	<b>0.077</b>	<b>0.151</b>	<b>0.216</b>	<b>105.263</b>	<b>10.961</b>	<b>4.023</b>
Rat (GT)	0.396	0.639	0.802	0.057	2.609	11.625
<b>Rat (Ours)</b>	<b>0.243</b>	<b>0.385</b>	<b>0.482</b>	<b>0.495</b>	<b>6.247</b>	<b>11.592</b>
Reindeer (GT)	0.580	0.833	0.918	0.020	2.177	14.077
<b>Reindeer (Ours)</b>	<b>0.043</b>	<b>0.073</b>	<b>0.106</b>	<b>130.645</b>	<b>11.970</b>	<b>2.953</b>

Table 4: Continued from Table 3.

Method	R-Prec Top 1 $\uparrow$	R-Prec Top 2 $\uparrow$	R-Prec Top 3 $\uparrow$	FID $\downarrow$	MultiModal-Dist $\downarrow$	Diversity $\rightarrow$
Rhino (GT)	0.349	0.575	0.690	0.031	2.971	10.070
<b>Rhino (Ours)</b>	<b>0.055</b>	<b>0.106</b>	<b>0.147</b>	<b>60.834</b>	<b>8.572</b>	<b>3.423</b>
Roach (GT)	0.516	0.693	0.828	0.014	2.456	12.001
<b>Roach (Ours)</b>	<b>0.047</b>	<b>0.120</b>	<b>0.182</b>	<b>56.589</b>	<b>9.980</b>	<b>5.248</b>
Sabre-toothed tiger (GT)	0.625	0.795	0.867	0.029	2.804	10.963
<b>Sabre-toothed Tiger (Ours)</b>	<b>0.035</b>	<b>0.071</b>	<b>0.098</b>	<b>18.381</b>	<b>8.898</b>	<b>5.478</b>
Sand mouse (GT)	0.373	0.595	0.742	0.007	2.878	11.316
<b>Sand Mouse (Ours)</b>	<b>0.035</b>	<b>0.067</b>	<b>0.118</b>	<b>65.683</b>	<b>9.128</b>	<b>3.479</b>
Scorpion (GT)	0.548	0.772	0.888	0.022	1.702	12.928
<b>Scorpion (Ours)</b>	<b>0.048</b>	<b>0.809</b>	<b>0.108</b>	<b>63.289</b>	<b>10.349</b>	<b>4.709</b>
Shark (GT)	0.412	0.627	0.760	0.022	3.118	9.744
<b>Shark (Ours)</b>	<b>0.210</b>	<b>0.335</b>	<b>0.387</b>	<b>0.568</b>	<b>7.090</b>	<b>9.415</b>
Skunk (GT)	0.484	0.712	0.786	0.021	2.615	11.999
<b>Skunk (Ours)</b>	<b>0.022</b>	<b>0.056</b>	<b>0.094</b>	<b>81.971</b>	<b>10.250</b>	<b>3.155</b>
Spider (GT)	0.373	0.618	0.752	0.007	2.279	12.354
<b>Spider (Ours)</b>	<b>0.060</b>	<b>0.103</b>	<b>0.150</b>	<b>81.980</b>	<b>10.375</b>	<b>2.722</b>
Stegosaurus (GT)	0.371	0.573	0.706	0.049	2.976	10.145
<b>Stegosaurus (Ours)</b>	<b>0.042</b>	<b>0.073</b>	<b>0.113</b>	<b>59.360</b>	<b>7.915</b>	<b>1.001</b>
T-Rex (GT)	0.125	0.250	0.344	0.163	4.367	5.915
<b>T-Rex (Ours)</b>	<b>0.000</b>	<b>0.031</b>	<b>0.063</b>	<b>31.338</b>	<b>7.166</b>	<b>2.823</b>
Tricera (GT)	0.316	0.502	0.625	0.004	3.626	10.532
<b>Tricera (Ours)</b>	<b>0.047</b>	<b>0.090</b>	<b>0.137</b>	<b>62.515</b>	<b>8.280</b>	<b>1.059</b>
Toucan (GT)	0.489	0.723	0.842	0.012	2.457	13.668
<b>Toucan (Ours)</b>	<b>0.205</b>	<b>0.364</b>	<b>0.464</b>	<b>0.915</b>	<b>7.441</b>	<b>12.437</b>
Turtle (GT)	0.426	0.665	0.790	0.016	2.266	11.510
<b>Turtle (Ours)</b>	<b>0.036</b>	<b>0.078</b>	<b>0.123</b>	<b>64.208</b>	<b>8.913</b>	<b>2.299</b>
Tyrannosaurus Rex (GT)	0.425	0.681	0.799	0.007	1.606	11.587
<b>Tyrannosaurus Rex (Ours)</b>	<b>0.054</b>	<b>0.087</b>	<b>0.144</b>	<b>68.680</b>	<b>8.512</b>	<b>1.638</b>
Wyvern (GT)	0.424	0.643	0.750	0.077	2.693	11.574
<b>Wyvern (Ours)</b>	<b>0.098</b>	<b>0.196</b>	<b>0.290</b>	<b>43.339</b>	<b>8.184</b>	<b>4.517</b>
Average (GT)	0.437	0.650	0.767	0.024	2.559	11.790
<b>Average (Ours)</b>	<b>0.069</b>	<b>0.144</b>	<b>0.173</b>	<b>62.785</b>	<b>9.371</b>	<b>4.158</b>

with no significant criticisms regarding their quality. The results were notably impressive, with many participants expressing enthusiasm for widespread use of these animations.

This comprehensive user study confirms that our animations not only meet but exceed user expectations in terms of quality, realism, and engagement, making them highly suitable for varied practical applications. The insights from this study will guide further enhancements to ensure our animation generation remains at the forefront of technological and artistic innovation.

The figure displays a user interface for a study. It is organized into four rows, each corresponding to a video prompt. Each row contains a video player on the left and a set of evaluation questions on the right.

- Video A:** Prompt: "a man is jumping in place". The video player shows a man jumping. The evaluation question is: "Rate the accuracy and naturalness of the motion depicted in each video on a scale from 1 to 5, where 1 indicates 'Very Inaccurate' and 5 indicates 'Very Natural'." The scale has five radio buttons labeled 1, 2, 3, 4, 5.
- Video B:** Prompt: "A person stands, crosses left leg in front of the right, lowering themselves until they are sitting". The video player shows a person performing this action. The evaluation question is: "Evaluate the visual quality and detail of the mesh used in the animations. How well are the textures and models rendered? Please rate from 1 (Poor Quality) to 5 (Excellent Quality)". The scale has five radio buttons labeled 1, 2, 3, 4, 5.
- Video C:** Prompt: "a man raised up his hand and shake in place". The video player shows a man raising his hand and shaking. The evaluation question is: "How seamlessly do the motion and mesh combine in the animations? Rate the integration on a scale of 1 (Poor Integration) to 5 (Flawless Integration)". The scale has five radio buttons labeled 1, 2, 3, 4, 5.
- Video D:** Prompt: "a man is kicking a ball in place". The video player shows a man kicking a ball. The evaluation question is: "Reflect on your overall feelings towards the animations. How engaging and appealing did you find them? Rate your experience from 1 (Not Engaging) to 5 (Highly Engaging)". The scale has five radio buttons labeled 1, 2, 3, 4, 5.

At the bottom of the interface, there are two buttons: "Submit" and "Clear form".

Figure 5: This figure displays the User Interface (UI) used in our User Study, showcasing four videos (Video A to D) each with distinct motion animations from various models. Participants evaluate these animations on aspects such as motion accuracy, mesh quality, integration of motion and mesh, and overall user experience. They rate each aspect from 1 (low) to 5 (high) to assess how the animations mirror real-world movements, the visual appeal of the animations, their integration quality, and their engagement level. This evaluation aims to determine the realism and engagement effectiveness of each animation model.

## C Avatar Q&A Dataset Example

```
1 {
2   {
3     "instruction": "I saw an animal attacking something. A closer look makes it clear that
4     a monkey is attacking",
5     "input": "",
6     "output": "The animal is (Monkey), and motion is (Attack).",
7     "history": []
8   },
9   {
10    "instruction": "A chicken walked quickly from my line of sight",
11    "input": "",
12    "output": "The animal is (Chicken), and motion is (Walk Quick).",
13    "history": []
14  },
15  {
16    "instruction": "A fox, seeing the food ahead, lowers its body and slowly approaches
17    its prey",
18    "input": "",
19    "output": "The animal is (Fox), and motion is (Low Bite).",
20    "history": []
21  },
22  {
23    "instruction": "A fox walked out of the woods.",
24    "input": "",
25    "output": "The animal is (Fox), and motion is (Walk Out).",
26    "history": []
27  },
28  {
29    "instruction": "The rabbit hopped across the meadow, its fluffy tail bouncing in the
30    sunlight.",
31    "input": "",
32    "output": "The animal is (Rabbit), and motion is (Hop).",
33    "history": []
34  }
35 }
```

Listing 1: Examples from the Avatar Q&A Dataset